Zircon Record of Supercontinent Amalgamation in Back-arc Volcanic Rocks

Zhigang Zeng (zgzeng@ms.qdio.ac.cn)
Institute of Oceanology, Chinese Academy of Sciences

Zuxing Chen
Institute of Oceanology, Chinese Academy of Sciences

Yuxiang Zhang
Institute of Oceanology, Chinese Academy of Sciences

Research Article

Keywords: Episodic supercontinental amalgamation, zircons in volcanic rocks, supercontinental amalgamation events

Posted Date: November 24th, 2020

DOI: https://doi.org/10.21203/rs.3.rs-109172/v1

Abstract

Episodic supercontinental amalgamation has profoundly influenced the evolution of the geosphere, hydrosphere, atmosphere and biosphere. However, the timing of supercontinent formation has mainly been constrained by the global age spectra of detrital zircon. Here, we show that the zircons in back-arc volcanic rocks not only reflect the evolution of local magmatism but also contain a record of global continental amalgamation events. We found that the young (<100 ka) zircons in volcanic rocks from the Okinawa Trough have old (108 Ma to 2.7 Ga) inherited zircon, which were captured as the magma ascended through the rifting continental crust. Moreover, the ages of the inherited zircons correspond to five supercontinent amalgamation events. Specifically, the Archaean inherited zircons, which have positive $\varepsilon Hf_{(t)}$ and low $\delta^{18}O$ values, correspond to the formation of juvenile global continental crust. In contrast, the negative $\varepsilon Hf_{(t)}$ and high $\delta^{18}O$ values of post-Archaean inherited zircons indicate that their parental magma contained recycled, old crust due to the enhanced crustal thickening and crust-mantle interactions during supercontinent assembly. Therefore, inherited zircons in back-arc volcanic rocks not only reflect the evolution of local magmatism but also contain a record of global supercontinental amalgamation events.

Introduction

The history of episodic supercontinent amalgamation and dispersal has profoundly influenced Earth processes, surface environments and biogeochemical cycles[1-3]. Since zircons are physicochemically robust, accumulate as common accessory phases in sedimentary detritus[4], and can be isotopically dated through the U and Th decay systems, thereby resolving timescales from gigayears (Ga) to kiloyears (ka)[5-6], the timing of supercontinent formation was mainly constrained by the global age spectra of detrital zircon from the world's rivers[1,2]. Based on the distinct peaks of global U-Th-Pb ages in detrital zircon, the timing of assembly of the Kenorland, Nuna, Rodinia, Gondwana and Pangaea supercontinents has been revealed[1,2,7]. At present, however, no studies have reported records of these five global supercontinent amalgamation events in zircons from local back-arc volcanic eruptions. In this study, we used magmatic zircons, captured from the deep crust during mantle-derived magma ascent through the rifting upper crust in the Okinawa Trough (OT) to analyse the era of magmatic activity in this region and provide information about global supercontinental amalgamation events.

The OT, which is located on the western Pacific active continental margin (Fig. S1), is a back-arc basin formed by the northwestward subduction of the Philippine Sea Plate beneath the Eurasian Plate initiating during the middle to late Miocene (i.e., from >15 Ma to ~6 Ma)[8]. The crustal thickness decreases from >25 km in the northern OT to ~10 km on the axis of the SOT graben[9]. The southernmost part of the OT (SPOT), which is considered an embryonic crustal rifting zone where the crust (25–30 km) has not experienced significant thinning[10], is characterized by a cluster of active volcanoes dominated by dacites and rhyolites[10,11]. These <0.2 Ma silicic magmas evolved via mixing of a mantle-derived basaltic magma and a crustal felsic magma, followed by extensive fractional crystallization[10,11].

Zircons were separated from the three submarine volcanic rock samples at the three stations (C1, T9 and R10-H2; Figs. S1 and S2), which are calc-alkalic rhyolites and dacite (Fig. S3) and have the most isotopically enriched compositions of all the volcanic rocks in the OT (Fig. S4). We used secondary ionization mass spectrometry (SIMS), laser ablation multicollector inductively coupled mass spectrometry (LA-MC-ICP-MS), and cathodoluminescence (CL) imaging to investigate the U-Th-Pb-O-Hf isotope and trace element compositions of Quaternary zircons and old zircon cores captured from the deep crust during mantle-derived magma ascent through the rifting continental crust in the southern Okinawa Trough (SOT). We used these data to investigate the era of magmatic activity in this region and to provide information on global supercontinent amalgamation events.

Results

U-Th-Pb Ages

We used CL imaging to identify light-CL zircons (LCLZs) with dark-CL zircon cores (DCLZs) in the samples (Fig. S5). The LCLZs are in U-Th radioactive disequilibrium (Fig. S6), and the U-Th ages (<100 ka) of the LCLZs from the rhyolites and the dacite are similar and coeval (Fig. 1A). The cumulative probability density function (PDF) curve peaks at 30 ka for the LCLZs in the rhyolites, whereas the PDF curve peaks at 19 and 45 ka for the LCLZs in the dacite (Fig. 1B). In contrast to the LCLZs, the DCLZs in both the dacite and the rhyolites are older (U-Pb ages of 108 Ma to 2.7 Ga) (Figs. 2 and S5; Table S2), and the age distribution of the DCLZs (Table S2) is consistent with the ages of the five supercontinent amalgamation events (Fig. 2).

Hf-O isotopes

In contrast to the DCLZs (Fig. 2; Table S2), the LCLZs have narrow $\delta^{18}O$ and $\varepsilon Hf_{(t)}$ ranges (Figs. 2 and S7; Table S1). Seven relatively large DCLZs have $\varepsilon Hf_{(0)}$ values of −54.5 to −6.8, which correspond to $\varepsilon Hf_{(t)}$ values of −15.7 to +4.9 and two-stage crustal Hf model ages (T_{DM2}) of 1419–2837 Ma (Figs. 2 and S5; Table S2). In contrast to the Proterozoic and Phanerozoic zircons (Fig. 2), the $\varepsilon Hf_{(t)}$ values of the ~2.7 Ga Archaean DCLZs are positive.

Trace elements

The LCLZs have high Th/U ratios (0.4–1.0; Fig. S8; Table S3). The Ti contents of the LCLZs of rhyolites, R10-H2 and T9', and dacite, C1, are 5.6–58.6 ppm, 3.9–110.7 ppm, and 5.1–48.0 ppm, respectively; they have Ti-in-zircon temperatures of 693–924°C, 664–1008°C, and 685–900°C, respectively (Table S3). All of the LCLZs have steep chondrite-normalized rare earth element (REE) patterns with variable heavy REE (HREE) enrichments, prominent positive Ce anomalies, and strong negative Eu anomalies (Fig. S9). The DCLZs are less HREE enriched and do not have significant Eu anomalies (Fig. 3; Table S3).

Discussion

Long-lived silicic magma reservoirs beneath the OT

The LCLZs are euhedral with oscillatory zoning (Fig. 1A) and have high Th/U ratios (>0.4; Fig. S8), exhibiting steep chondrite-normalized REE patterns with variable HREE enrichments, prominent positive Ce anomalies, and strong negative Eu anomalies (Fig. S9), which are characteristic of magmatic zircons[12], indicating a magmatic origin rather than a detrital or metamorphic origin[12-13]. Moreover, the LCLZs exhibit homogeneous $\delta^{18}O$ and $\varepsilon Hf_{(t)}$ values (Figs. 2 and S7), suggesting that all the LCLZs crystallized from their parent magma[14]. The crystallization temperatures decrease systematically with increasing Hf concentration (Fig. S10), which is a fractionation proxy[15], suggesting that the decrease in temperature was accompanied by protracted zircon crystallization. Multiple age spots on individual LCLZs with continuous and uninterrupted oscillatory zoning (Fig. 1A) revealed age differences of up to 85 ka between the core and rim domains, providing further evidence of protracted zircon crystallization. Overall, the LCLZs crystallized in a long-lived upper crustal magma reservoir for ~100 ka, which is consistent with the results of other studies conducted on the longevity of silicic magma systems in continental arc settings [15]. The outermost crystal rims represent the youngest phase of zircon crystallization (1.8 +3.6/−3.5 ka) (Fig. 1; Table S1). We interpret this to be the approximate eruption age. Chen et al.[16] and Huang et al.[17] obtained U-series ages of 88.7–12.7 ka for the silicic rocks from the middle and northern OT. These ages suggest that volcanic activity has occurred throughout the OT since the Late Pleistocene[16,17]. This volcanic activity was likely sustained by long-lived silicic magma reservoirs beneath the submarine volcanoes [15].

Provenance of the zircon xenocryst cores in the silicic magmas

A prominent feature observed in this study is that some of the LCLZs in the volcanic rocks had DCLZs with U-Pb ages of ~108 Ma to 2.7 Ga (Fig. S5; Table S2). Based on the Hf-O isotope compositions of the LCLZs, the Quaternary volcanic rocks were likely produced by the mixing of a mantle-derived mafic magma with ~10–20% crust-derived silicic magma (Figs. S7C -7D), which is supported by the enriched radiogenic Sr-Nd isotope compositions of the whole-rock samples[11] (Fig. S4). The involvement of a high percentage of a crustal component is consistent with the presence of inherited ancient zircons (the DCLZs) with rim overgrowths (the LCLZs)[18] (Fig. S5). The presence of the DCLZs in the subduction-related volcanic rocks is either due to the direct incorporation of the DCLZs into the mantle source via subducted sediment[19, 20] or the capture of fragments of ancient continental crust (containing the DCLZs) during magma ascent[21-23]. Experimental results have demonstrated that the retention times of O isotopes in 20–120 μm zircons at a temperature of 900°C are between 160 and 5700 years [24]. For hotter mantle magmas, the time required for the $\delta^{18}O$ to reach diffusive equilibrium with the homogeneous mantle value is much shorter than 5.7 ka[25]. The high saturation level of mafic melts causes the fast dissolution of pre-existing zircons under normal conditions[26]. Thus, it would not be possible for continent-derived zircon crystals that have been recycled back into the mantle by subduction to preserve highly variable O isotope signatures at mantle temperatures[25]. Therefore, the DCLZs with highly variable $\delta^{18}O$ values (Fig.

2) must be remnants of a deeply buried basement that underwent extensive partial melting by and mixing with the ascending magma. In other words, these DCLZs are unmelted remnants of the basement.

Remnants of the Cathaysian Block underlying the embryonic crustal rifting zone

During this study, Archean zircon cores were found in both the dacite and the rhyolites. The Archaean DCLZs have the following characteristics. (1) They exhibit clear, bright, and broad oscillatory zoning in the CL images and euhedral to subhedral rather than oval shapes (Fig. 3A), indicating that these zircons are magmatic rather than detrital. (2) They have high Th/U ratios of 0.59 (Table S3), suggesting a magmatic rather than a metamorphic origin (Th/U<0.1)[13]. (3) They lack significant Eu anomalies, exhibit relatively flat HREE patterns (Fig. 3B), and have lower contents of incompatible elements, such as Y, Hf, and U, than the younger zircon rims (Table S3), suggesting that they crystallized from a less evolved magma[12]. (4) They have oxygen isotope compositions (5.74–5.85‰; Fig. 2B; Table S2) similar to those of mantle zircons (5.3 ± 0.3‰)[27] and positive $\varepsilon Hf_{(t)}$ values (4.66 to 4.88; Table S2) that plot between the evolutionary trends of the depleted mantle[28] and chondrites[29] (Fig. 3C), suggesting that the parent rocks of the DCLZs were mainly derived from the depleted mantle. (5) They have $\varepsilon Hf_{(t)}$ values within the lower crustal range[30] (Fig. 3C). Collectively, these lines of evidence suggest that the Archaean DCLZs were derived from a mafic source that was extracted from the basaltic lower crust of the SPOT, which formed through melting of the depleted mantle ~2.9 Ga (Fig. 3C).

In addition, drilling results show that the 174 Ma granitoids in the adjacent East China Sea Basin (Fig. 4A) have crustal Hf model ages of 2.9–2.5 Ga, implying that their parent magmas were derived from reworking of the Archaean lower crust[31]. Similarly, the Archaean zircons (2.7–2.5 Ga) in the studied volcanic rocks suggest the presence of unexposed Archaean lower crust beneath the SPOT (Fig. 4B). The ages and Hf isotope compositions of these zircons are also similar to the zircons found in the lower crustal xenoliths in the western Cathaysia Block, southern China (Fig. 4A)[32]. Moreover, one DCLZ with a Neoproterozoic age (741.7 Ma) had a very low $\varepsilon Hf_{(t)}$ value (−15.7) and an Hf model age (T_{DM2}) of 2.6 Ga (Table S2), indicating that its parent magma was derived from the reworking of Archaean crust. Inherited zircons with a Cathaysian affinity are also abundant in the young igneous rocks of the adjacent Luzon arc[21]. Thus, the inherited Archean zircons in the volcanic rocks strongly suggest that remnants of the old Cathaysian Block underlie the embryonic crustal rifting zone in the SPOT. In contrast to the Archaean samples, one Neoproterozoic DCLZ (1.0 Ga) and three Mesozoic DCLZs (150.9–237.5 Ma) exhibit slightly negative $\varepsilon Hf_{(t)}$ values (−3.3 to −5.7) and Proterozoic Hf model ages (T_{DM2} = 1.4–2.2 Ga; Table S2), suggesting that their parent magmas were derived from the reworking of Proterozoic crustal components or from mixing of crust-derived magmas and juvenile material[28]. Thus, the older basement has experienced reworking and complex modification related to the addition of juvenile material since the Neoarchean. In addition, their highly variable $\delta^{18}O$ values suggest that they may have originated from the metasedimentary basement in the upper and middle crust overlying the Archean crystalline basement of the lower crust (Fig. 4B).

Implications for the timing of continent amalgamation events

Notably, the age distribution of the DCLZs coincides with five supercontinent amalgamation events (Fig. 2). We propose that the Archaean DCLZs (2.5–2.7 Ga), with positive εHf(t) values and low oxygen isotope values (5.74–5.85‰) (Fig. 2; Table S2), are unique and related to the formation of juvenile continental crust, i.e., crust that segregated rapidly from the mantle without significant involvement of older crustal materials[33]. This event occurred during the amalgamation of Kenorland and is the largest global event that affected volcanism on all continents[34]. The ages of the post-Archaean DCLZs fall within the periods of supercontinent assembly at ~2.1–1.7 Ga (Nuna), 1.3–0.95 Ga (Rodinia), 0.7–0.5 Ga (Gondwana), and 0.35–0.18 Ga (Pangea) (Fig. 2)[1,2,35]. The negative $\varepsilon Hf_{(t)}$ values of these DCLZs indicate that their parent magmas contained recycled older crust[28]. This interpretation may be consistent with the fact that the crustal thickening caused by supercontinent assembly results in more crust-mantle interaction[36]. As such, the DCLZs from the OT act as a record of global continental amalgamation events. DCLZs have also been found in other subduction-related volcanic rocks[21-23], making these records an essential tool for improving our understanding of the supercontinent cycle and the amalgamation process.

Conclusions

In summary, zircon U-Th-Pb ages and trace elements as well as Hf-O isotopes results support the following model for the two silicic magma eruptions from the southwest OT: (1) long-lived magma reservoirs beneath the submarine volcanos with a protracted time scale at least 100 ky; (2) Zircon xenocrysts acquired during the magma ascent through the upper crust rather than recycled from the subducted sediments; (3) The occurrence of these Archean zircon suggests the presence of unexposed Archean materials in the southern OT crust, which experienced complex modification related to the addition of juvenile material and reworking from Neoarchean time onward; (4) The Archean zircon xenocryst cores correspond to the global formation event of “juvenile” continental crust. Post-Archean zircon xenocryst cores indicate their parent magma contains recycled older crustal material. This may consistent with the fact that crustal thickening result in crust-mantle interaction during supercontinent assembly. Therefore, zircons in back-arc volcanic rocks not only reflect the local evolution of continents, but also record the global continental amalgamation. In the future, the study of zircon from other back-arc volcanic rocks in the western Pacific is expected to find zircons that record the supercontinent cycle and amalgamation.

Methods

Zircons were separated from the three volcanic rock samples (Fig. S2). Representative zircon grains were mounted in epoxy resin and polished to expose grain centers. For all epoxy mounts of zircon grains, cathodoluminescence (CL) images were obtained prior to analysis, and used to guide the analysis locations. First, secondary ion mass spectrometry (SIMS) analyses were performed for zircon U-Th-Pb-O

isotopes and trace elements. The same grains of zircon were then analyzed by LA-MC-ICPMS for a determination of Lu-Hf isotopes.

Zircon ^{238}U-^{230}Th disequilibrium ages and trace element compositions were obtained by SIMS using a CAMECA IMS 1270 at the University of California Los Angeles (UCLA) following the analytical protocols described by Schmitt et al.[37] and Bell and Harrison[38]. Zircon U-Pb and O analyses were performed using a CAMECA IMS 1280 at the Institute of Geology and Geophysics, Chinese Academy of Sciences (IGGCAS), following the analytical procedure described by Li et al.[39] and Tang et al.[40]. Finally, zircon in situ Hf isotope analysis was carried out using LA-MC-ICP-MS at Nanjing University, China. Details of analytical methods and data of zircon U-Th-Pb-O-Hf isotopes and trace elements are available in Supplementary materials.

Declarations

Data availability

All data are reported in the Supplementary Information.

Acknowledgments

We would like to thank the crews of the R/V KEXUE during the HOBAB 3 and 4 cruises for their help with sample collection. We are grateful to Xianhua Li and Qiuli Li at IGGCAS, and Ming-Chang Liu and Elizabeth Bell at UCLA for their assistance with the SIMS analyses. This work was supported by the NSFC (91958213), the International Partnership Program of Chinese Academy of Sciences (133137KYSB20170003), and the Taishan Scholar Foundation of Shandong Province (ts201511061).

Author contributions statement

Z.G.Z. defined the research theme, analysed the data, interpreted the results and wrote the paper. Z.X.C. analysed the data, interpreted the results and wrote the paper. Y.X.Z. analysed the data. Z.G.Z. and Z.X.C. designed the methods. Z.G.Z., Z.X.C. and Y.X.Z conducted, discussed, interpreted, and presented the SEM, SIMS and LA-MC-ICP-MS analyses.

Competing interests

The authors declare no competing interests.

References

1. Campbell, I. H. & Allen, C. M. Formation of supercontinents linked to increases in atmospheric oxygen. *Nature Geosci.* **1**, 554-558 (2008).
2. Bradley, D. C. Secular trends in the geologic record and the supercontinent cycle. *Earth Sci. Rev.* **108**, 16-33 (2011).

3. Nance, R. D., Murphy, J. B. & Santosh, M. The supercontinent cycle: A retrospective essay. *Gondwana Research* **25**, 4-29 (2014).
4. Barham, M., Kirkland, C. L. & Hollis, J. Spot the difference: Zircon disparity tracks crustal evolution. *Geology* **47**, 435-439 (2019).
5. Keller, C. B., Boehnke, P. & Schoene, B. Temporal variation in relative zircon abundance throughout Earth history. *Geochem Perspect Lett* **3**, 179-189 (2017).
6. Schmitt, A. K. Uranium series accessory crystal dating of magmatic processes. *Annu. Rev. Earth. Planet. Sci.* **39** (2011).
7. Spencer, C. J., Cawood, P. A., Hawkesworth, C. J., Raub, T. D., Prave, A. R., & Roberts, N. M. Proterozoic onset of crustal reworking and collisional tectonics: Reappraisal of the zircon oxygen isotope record. *Geology* **42**, 451-454 (2014).
8. Sibuet, J. C., Deffontaines, B., Hsu, S. K., Thareau, N., Le Formal, J. P., & Liu, C. S. Okinawa trough backarc basin- Early tectonic and magmatic evolution. *J. Geophys. Res: Solid Earth* **103**, 30245–30267 (1998).
9. Arai, R., Kodaira, S., Yuka, K., Takahashi, T., Miura, S., & Kaneda, Y. Crustal structure of the southern Okinawa Trough: Symmetrical rifting, submarine volcano, and potential mantle accretion in the continental back-arc basin. *J. Geophys. Res: Solid Earth* **122**, 622–641 (2017).
10. Chung, S. L., Wang, S. L., Shinjo, R., Lee, C. S. & Chen, C. H. Initiation of arc magmatism in an embryonic continental rifting zone of the southernmost part of Okinawa Trough. *Terra Nova* **12**, 225-230 (2000).
11. Chen, Z., Zeng, Z., Yin, X., Wang, X., Zhang, Y., Chen, S., Shu, Y., Guo, K., & Li, X. Petrogenesis of highly fractionated rhyolites in the southwestern Okinawa Trough: Constraints from whole-rock geochemistry data and Sr-Nd-Pb-O isotopes. *Geol. J.* **54**, 316–332 (2019).
12. Belousova, E., Griffin, W. L., O'Reilly, S. Y. & Fisher, N. Igneous zircon: trace element composition as an indicator of source rock type. *Contrib. Mineral. Petrol.* **143**, 602-622 (2002).
13. Hoskin, P. W. & Schaltegger, U. The composition of zircon and igneous and metamorphic petrogenesis. *Rev. Mineral. Geochem.* **53**, 27-62 (2003).
14. Wotzlaw, J. F., Bindeman, I. N., Watts, K. E., Schmitt, A. K., Caricchi, L., & Schaltegger, U. Linking rapid magma reservoir assembly and eruption trigger mechanisms at evolved yellowstone-type supervolcanoes. *Geology* **42**, 807–810 (2014).
15. Claiborne, L. L., Miller, C. F., Flanagan, D. M., Clynne, M. A. & Wooden, J. L. Zircon reveals protracted magma storage and recycling beneath Mount St. Helens. *Geology* **38**, 1011-1014 (2010).
16. Chen, L. R., Zhai, S. K., & Shen, S. X. Isotopic characteristics and dating of pumice in Okinawa Trough. *Science China (Series B)* **23**, 324–329 (1993).
17. Huang, P., Li, A., Hu, N., Fu, Y., & Ma, Z. Isotopic feature and uranium dating of the volcanic rocks in the Okinawa Trough. *Science China-earth Sciences* **49**, 375–383 (2006).

18. Pack, B., Schmitt, A. K., Roberge, J., Tenorio, F. G., & Damiata, B. N. Zircon xenocryst resorption and magmatic regrowth at El Chichón Volcano, Chiapas, Mexico. *J. Volcanol. Geotherm. Res.* **311**, 170–182 (2016).
19. Xu, Z., Zheng, Y. F. & Zhao, Z. F. Zircon evidence for incorporation of terrigenous sediments into the magma source of continental basalts. *Sci. Rep* **8**, 178 (2018).
20. Rojas-Agramonte, Y., Garcia-Casco, A., Kemp, A., Kröner, A., Proenza, J. A., Lázaro, C., & Liu, D. Recycling and transport of continental material through the mantle wedge above subduction zones: A Caribbean example. *Earth Planet. Sci. Lett.* **436**, 93-107 (2016).
21. Shao, W. Y., Chung, S. L., Chen, W. S., Lee, H. Y. & Xie, L. W. Old continental zircons from a young oceanic arc, eastern Taiwan: Implications for Luzon subduction initiation and Asian accretionary orogeny. *Geology* **43**, 479-482 (2015).
22. Tapster, S., Roberts, N., Petterson, M., Saunders, A. & Naden, J. From continent to intra-oceanic arc: Zircon xenocrysts record the crustal evolution of the Solomon island arc. *Geology* **42**, 1087-1090 (2014).
23. Smyth, H., Hamilton, P., Hall, R. & Kinny, P. The deep crust beneath island arcs: inherited zircons reveal a Gondwana continental fragment beneath East Java, Indonesia. *Earth Planet. Sci. Lett.* **258**, 269-282 (2007).
24. Cherniak, D. J. & Watson, E. B. Diffusion in zircon. *Rev. Mineral. Geochem.* **53**, 113-143 (2003).
25. Li, X. H., Abd El-Rahman, Y., Abu Anbar, M., Li, J., Ling, X. X., Wu, L. G., & Masoud, A. E. Old Continental Crust Underlying Juvenile Oceanic Arc: Evidence From Northern Arabian-Nubian Shield, Egypt. *Geophys. Res. Lett.* **45**, 3001-3008 (2018).
26. Watson, E. B. & Harrison, T. M. Zircon saturation revisited: temperature and composition effects in a variety of crustal magma types. *Earth Planet. Sci. Lett.* **64**, 295-304 (1983).
27. Valley, J. W., Kinny, P. D., Schulze, D. J. & Spicuzza, M. J. Zircon megacrysts from kimberlite: oxygen isotope variability among mantle melts. *Contrib. Mineral. Petrol.* **133**, 1-11 (1998).
28. Griffin, W., Pearson, N. J, Belousova, E., Jackson, S. E v., Van Achterbergh, E., O'Reilly, Suzanne Y., & Shee, S. R. The Hf isotope composition of cratonic mantle: LAM-MC-ICPMS analysis of zircon megacrysts in kimberlites. *Geochim. Cosmochim. Acta* **64**, 133–147 (2000).
29. Blichert-Toft, J. & Albarède, F. The Lu-Hf isotope geochemistry of chondrites and the evolution of the mantle-crust system. *Earth Planet. Sci. Lett.* **148**, 243-258 (1997).
30. Amelin, Y., Lee, D.-C., Halliday, A. N. & Pidgeon, R. T. Nature of the Earth's earliest crust from hafnium isotopes in single detrital zircons. *Nature* **399**, 252-255 (1999).
31. Yuan, W., Yang, Z., Zhao, X., Santosh, M. & Zhou, X. Early Jurassic granitoids from deep drill holes in the East China Sea Basin: implications for the initiation of Palaeo-Pacific tectono-magmatic cycle. *Int. Geol. Rev.* **60**, 813-824 (2018).
32. Li, X. Y., Zheng, J. P., Xiong, Q., Zhou, X. & Xiang, L. Triassic rejuvenation of unexposed Archean-Paleoproterozoic deep crust beneath the western Cathaysia block, South China. *Tectonophys.* **724**, 65-79 (2018).

33. Arndt, N. & Davaille, A. Episodic earth evolution. *Tectonophys.* **609**, 661-674 (2013).
34. Condie, K. C. Episodic continental growth and supercontinents: a mantle avalanche connection? *Earth Planet. Sci. Lett.* **163**, 97-108 (1998).
35. Cawood, P. A., Hawkesworth, C. & Dhuime, B. The continental record and the generation of continental crust. *Bulletin* **125**, 14-32 (2013).
36. Gardiner, N. J., Kirkland, C. L. & Van Kranendonk, M. J. The Juvenile Hafnium Isotope Signal as a Record of Supercontinent Cycles. *Sci. Rep* **6**, 38503 (2016).
37. Schmitt, A. K., Stockli, D. F. & Hausback, B. P. Eruption and magma crystallization ages of Las Tres Vírgenes (Baja California) constrained by combined 230Th/238U and (U–Th)/He dating of zircon. *J. Volcanol. Geotherm. Res.* **158**, 281-295 (2006).
38. Bell, E. A. & Harrison, T. M. Post-Hadean transitions in Jack Hills zircon provenance: A signal of the Late Heavy Bombardment? *Earth Planet. Sci. Lett.* **364**, 1-11 (2013).
39. Li, X. H., Liu, Y., Li, Q. L., Guo, C. H. & Chamberlain, K. R. Precise determination of Phanerozoic zircon Pb/Pb age by multicollector SIMS without external standardization. *Geochem. Geophys. Geosyst.* **10** (2009).
40. Tang, G. Q., Li, X. H., Li, Q. L., Liu, Y., Ling, X. X., & Yin, Q. Z. Deciphering the physical mechanism of the topography effect for oxygen isotope measurements using a Cameca IMS-1280 SIMS. *J. Anal. Atom. Spectrom.* **30**, 950-956 (2015).
41. Roberts, N. M. & Spencer, C. J. The zircon archive of continent formation through time. *Geol. Soc. Lond. Spec. Publ.* **389**, 197-225 (2015).
42. Isozaki, Y. A visage of early Paleozoic Japan: Geotectonic and paleobiogeographical significance of Greater South China. *Isl. Arc* **28**, e12296 (2019).

Figures

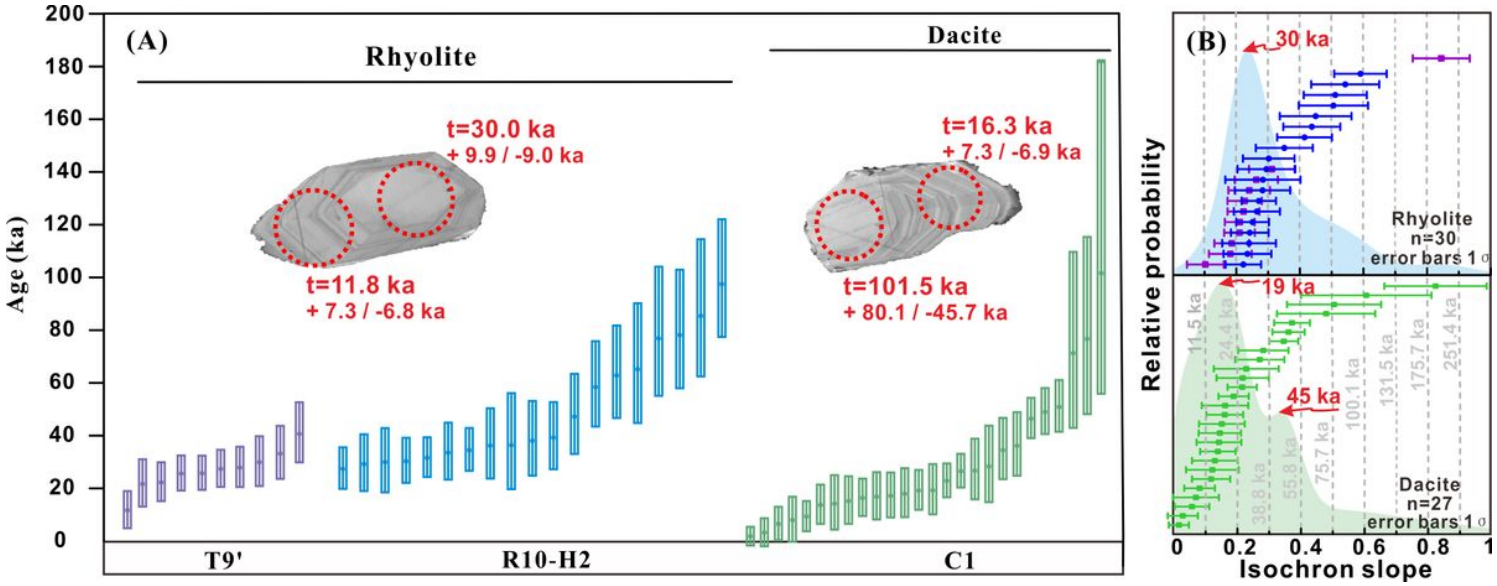

Figure 1

Zircon U-Th geochronology of the back-arc volcanic rocks. (a) CL images of two LCLZs showing several microprobe analysis locations and their corresponding ages. (b) Cumulative PDF curves of the slopes of the 238U-230Th model isochrons for the SIMS zircon data. The purple, blue, green and vertical dashed lines represent rhyolites T9', R10-H2, dacite C1 and reference ages.

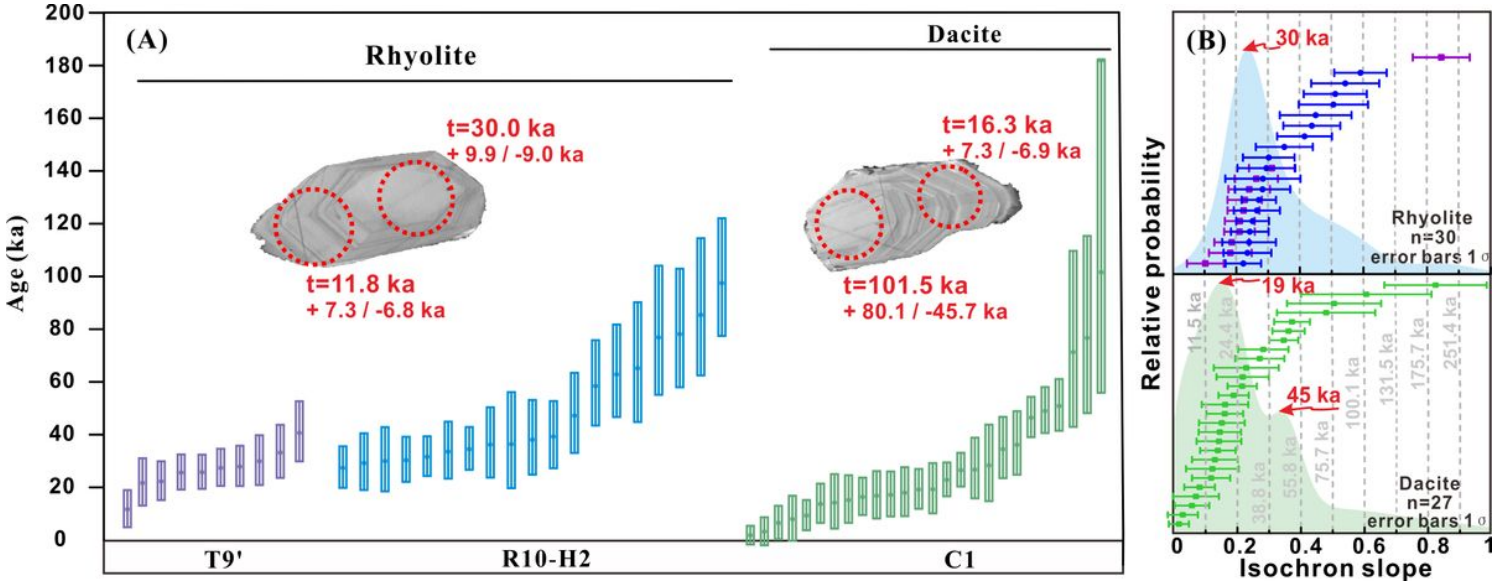

Figure 1

Zircon U-Th geochronology of the back-arc volcanic rocks. (a) CL images of two LCLZs showing several microprobe analysis locations and their corresponding ages. (b) Cumulative PDF curves of the slopes of the 238U-230Th model isochrons for the SIMS zircon data. The purple, blue, green and vertical dashed lines represent rhyolites T9', R10-H2, dacite C1 and reference ages.

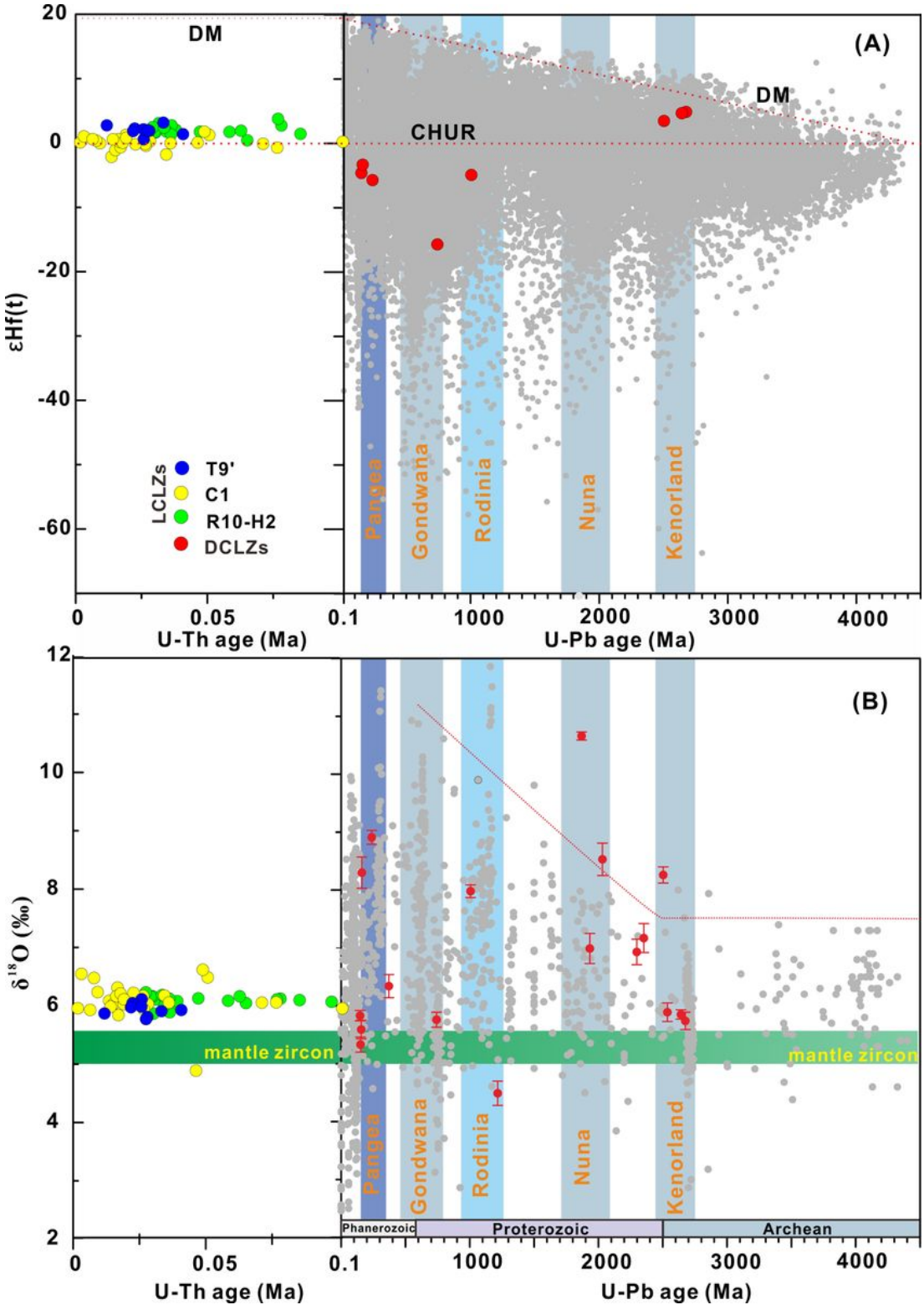

Figure 2

Plots of (a) εHf(t) and (b) δ18O vs. time for the LCLZs and DCLZs. The light grey dots represent global zircon εHf(t) (Roberts and Spencer, 41) and δ18O data (Spencer et al.7). The vertical bars represent supercontinent amalgamation events1,2,7.

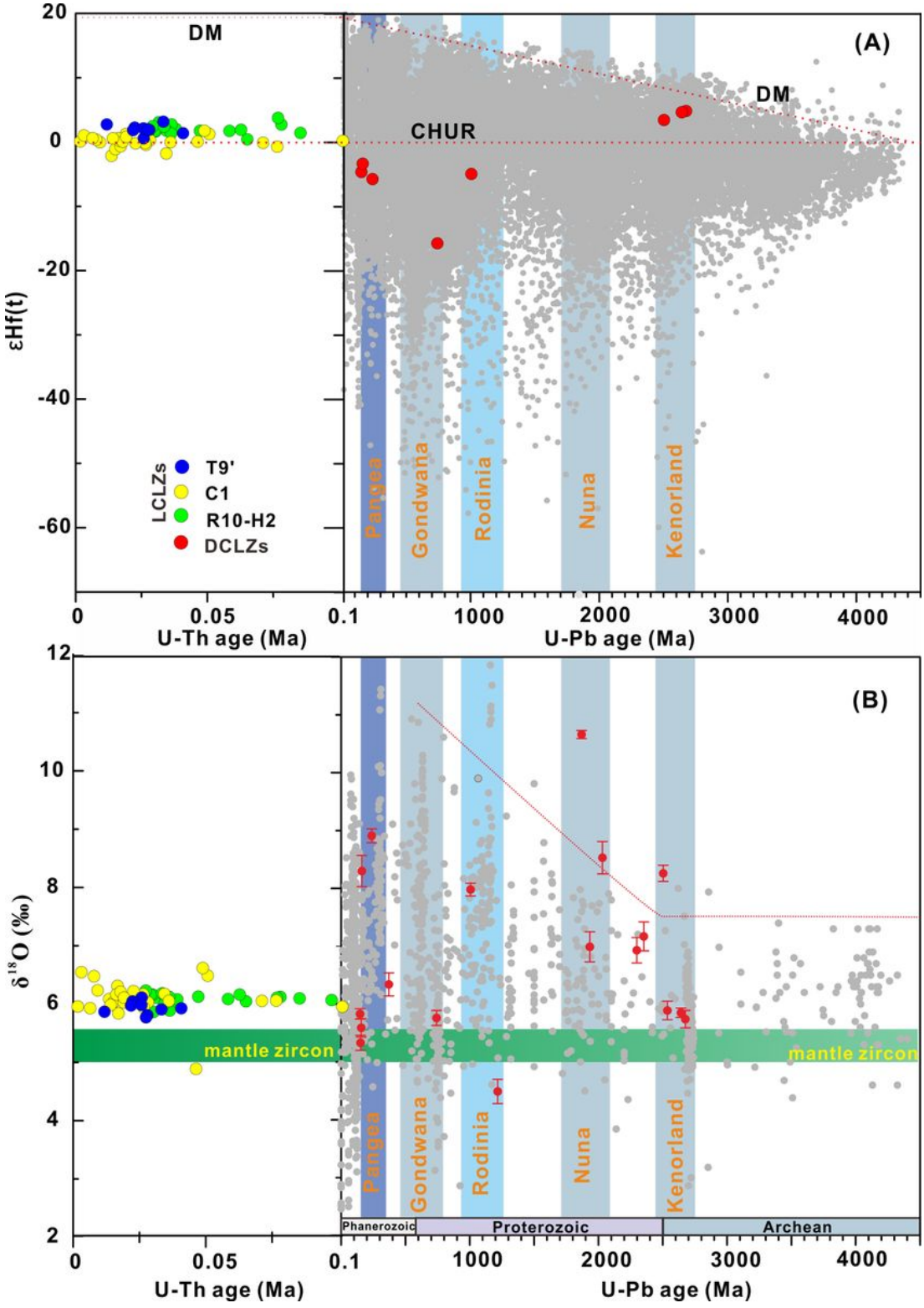

Figure 2

Plots of (a) εHf(t) and (b) δ18O vs. time for the LCLZs and DCLZs. The light grey dots represent global zircon εHf(t) (Roberts and Spencer, 41) and δ18O data (Spencer et al.7). The vertical bars represent supercontinent amalgamation events1,2,7.

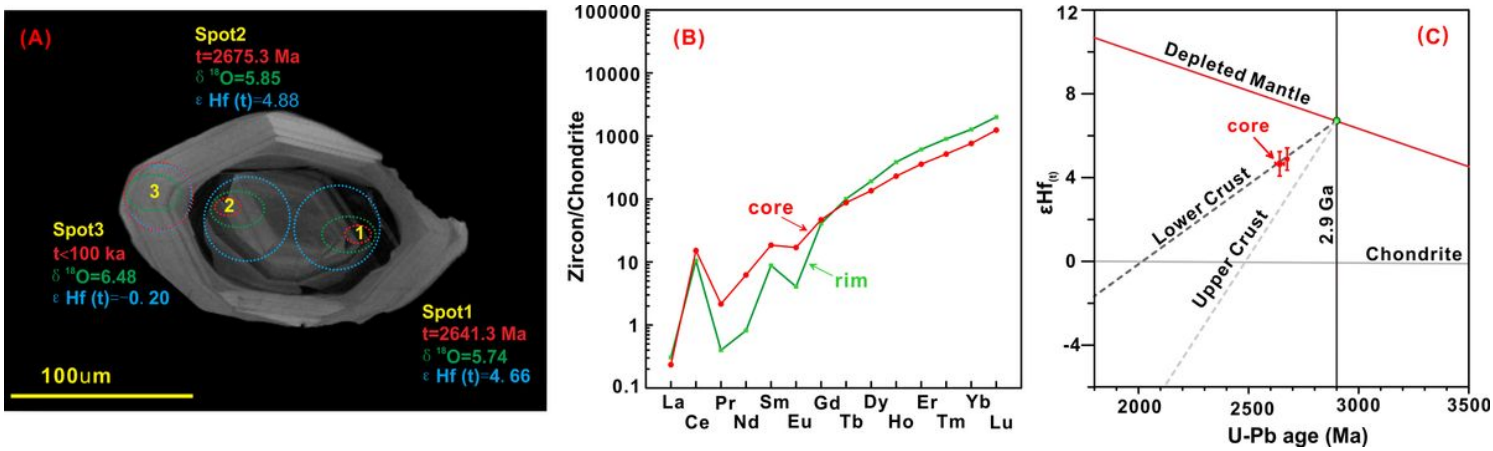

Figure 3

Representative LCLZ with a DCLZ core. (a) CL image of a zircon rim and core with the U-Th and U-Pb ages, δ18O and εHf(t) analysis locations and data shown. (b) REE diagram for the zircon's rim and core. C) Plot of εHf(t) vs. U-Pb age for the DCLZ cores. The εHf(t) values and ages of the geochemical reservoirs to Griffin et al.28, Blichert-Toft and Albarede29, Amelin et al.30.

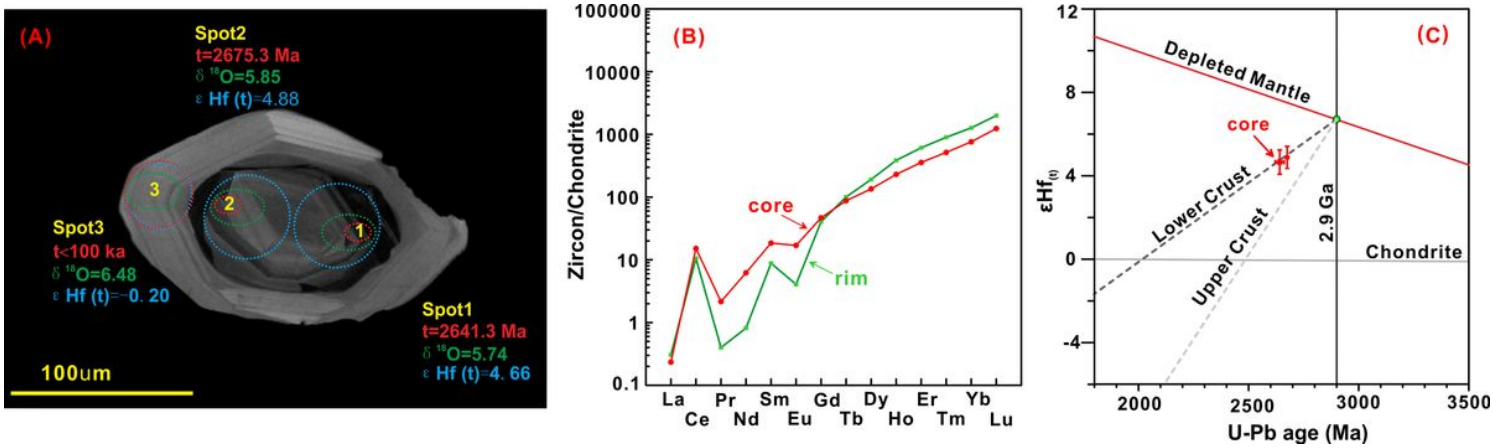

Figure 3

Representative LCLZ with a DCLZ core. (a) CL image of a zircon rim and core with the U-Th and U-Pb ages, δ18O and εHf(t) analysis locations and data shown. (b) REE diagram for the zircon's rim and core. C) Plot of εHf(t) vs. U-Pb age for the DCLZ cores. The εHf(t) values and ages of the geochemical reservoirs to Griffin et al.28, Blichert-Toft and Albarede29, Amelin et al.30.

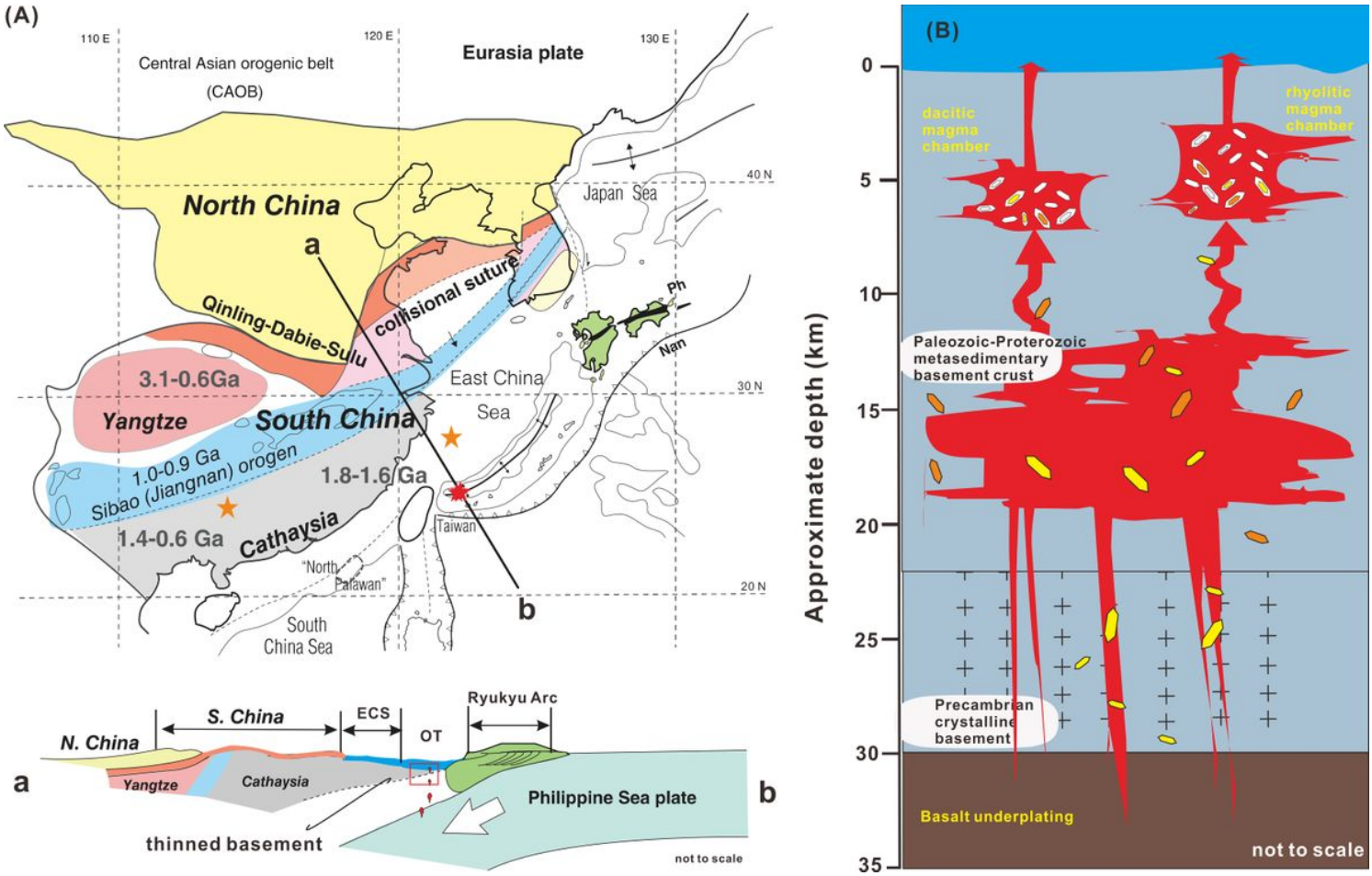

Figure 4

(a) The overall framework of adjacent, major continental blocks and schematic profile across the OT and China Block; modified from Isozaki42. The five-pointed stars show the sampling locations for this study, Li et al. 32 and Yuan et al.31. (b) The mantle-derived magma suffered crust assimilation, and xenocrystic zircons in the crust were carried by ascending magma to shallow magma chambers. Note: The designations employed and the presentation of the material on this map do not imply the expression of any opinion whatsoever on the part of Research Square concerning the legal status of any country, territory, city or area or of its authorities, or concerning the delimitation of its frontiers or boundaries. This map has been provided by the authors.

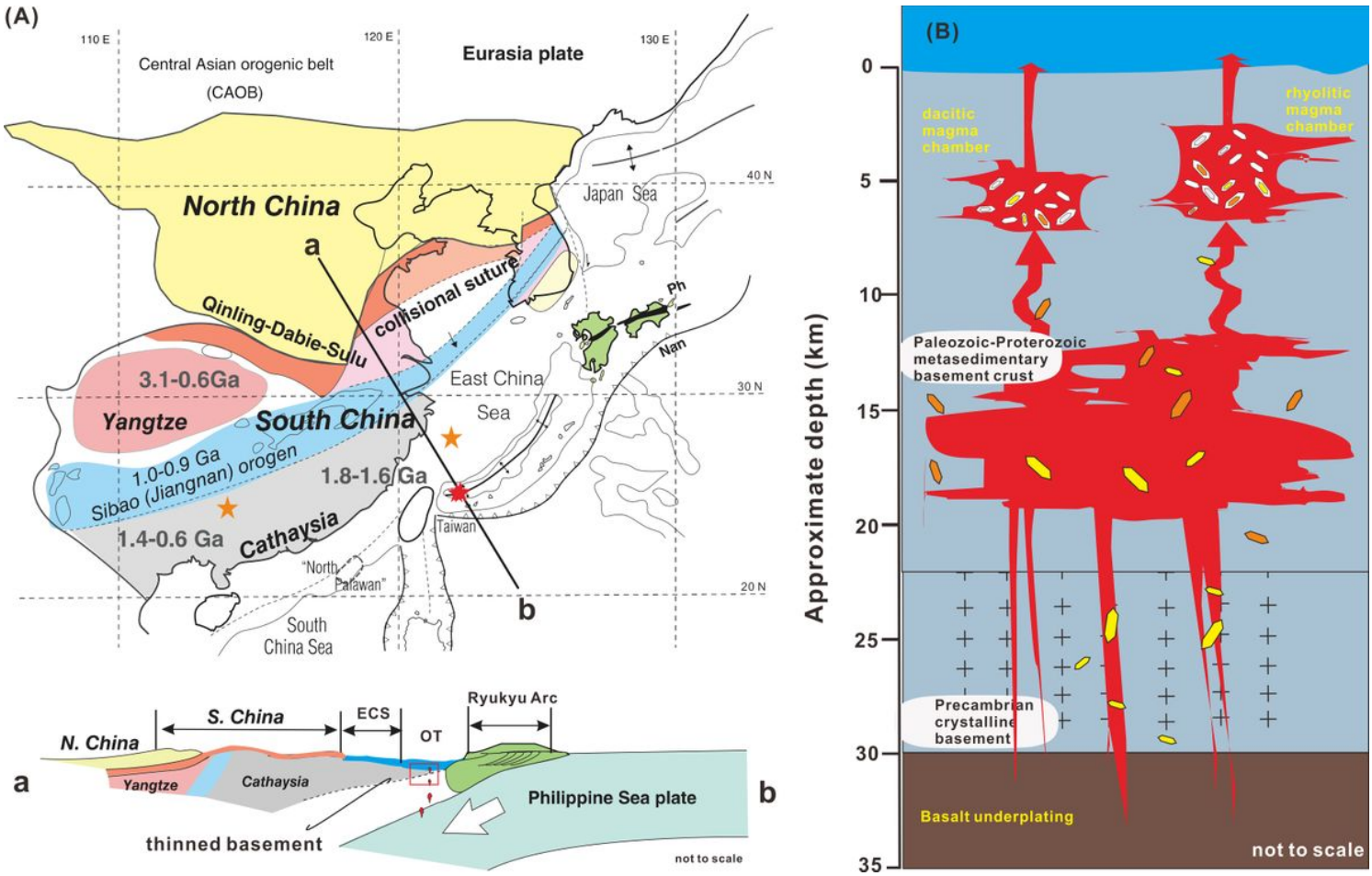

Figure 4

(a) The overall framework of adjacent, major continental blocks and schematic profile across the OT and China Block; modified from Isozaki42. The five-pointed stars show the sampling locations for this study, Li et al. 32 and Yuan et al.31. (b) The mantle-derived magma suffered crust assimilation, and xenocrystic zircons in the crust were carried by ascending magma to shallow magma chambers. Note: The designations employed and the presentation of the material on this map do not imply the expression of any opinion whatsoever on the part of Research Square concerning the legal status of any country, territory, city or area or of its authorities, or concerning the delimitation of its frontiers or boundaries. This map has been provided by the authors.

Supplementary Files

This is a list of supplementary files associated with this preprint. Click to download.

- Supplementaryinformation.pdf
- Supplementaryinformation.pdf